Laser-induced structural modifications of FeMoCuB metallic glasses before and after transformation into a nanocrystalline state

2001 J. Phys.: Condens. Matter 13 10359

(http://iopscience.iop.org/0953-8984/13/46/308)

INSTITUTE OF PHYSICS PUBLISHING JOURNAL OF PHYSICS: CONDENSED MATTER

J. Phys.: Condens. Matter **13** (2001) 10359–10369 PII: S0953-8984(01)27694-2

Laser-induced structural modifications of FeMoCuB metallic glasses before and after transformation into a nanocrystalline state

M Miglierini[1], P Schaaf[2], I Škorvánek[3], D Janičkovič[4], E Carpene[2] and S Wagner[2]

[1] Department of Nuclear Physics and Technology, Slovak University of Technology, Ilkovičova 3, 812 19 Bratislava, Slovakia
[2] Universität Göttingen, II. Physikalisches Institut, Bunsenstrasse 7/9, D-37073 Göttingen, Germany
[3] Institute of Experimental Physics, Slovak Academy of Sciences, Watsonova 47, 043 53 Košice, Slovakia
[4] Institute of Physics, Slovak Academy of Sciences, Dúbravská cesta 9, 842 28 Bratislava, Slovakia

Received 7 August 2001, in final form 1 October 2001
Published 2 November 2001
Online at stacks.iop.org/JPhysCM/13/10359

Abstract

The effects of laser treatments on the structural and magnetic properties of metallic ribbons have been studied using the melt-spun $Fe_{76}Mo_8Cu_1B_{15}$ alloy in as-quenched and nanocrystalline states. ^{57}Fe Mössbauer effect techniques, comprising transmission geometry measurements (TM) and detection of conversion electrons (CEMS), have been employed in addition to magnetization measurements, differential scanning calorimetry and x-ray diffraction. The Curie temperature of the as-quenched alloy was about 70 °C. The distributions of hyperfine magnetic fields as well as quadrupole splitting obtained from TM and CEM spectra have revealed the possibility of observing laser-induced structural modifications even at room temperature when the system is only weakly magnetic. Consequently, both types of hyperfine interactions have been detected and they are nearly in equilibrium (having the same strength or occurring to the same extent). After treatments with a pulsed XeCl excimer laser (with a homogeneous beam of 5×5 mm^2, 308 nm, 55 ns, 1 Hz), the significance of magnetic dipole interactions rises as a function of the number of laser pulses (up to 64) and the laser beam fluence (up to 3 J cm^{-2}). No traces of laser-induced crystallization have been found. In the nanocrystalline $Fe_{76}Mo_8Cu_1B_{15}$ alloy, surface crystallization was already completely removed after the first pulse of 1 J cm^{-2}.

1. Introduction

The use of lasers in industrial production processes provides a promising technology especially for treatment techniques. For example, nitriding is one of the methods of surface modification aiming to improve mechanical, tribological and chemical properties. In general, it requires high temperatures in order to incorporate nitrogen into steel or other iron-based alloys. This process can be effectively and rather simply accomplished by means of lasers—the so-called laser-nitriding [1].

During surface modification, magnetic properties of the treated material are also affected. Consequently, magnetically soft alloys such as metallic glasses are very sensitive to laser processing. On the other hand, this technique can be used to tailor not only mechanical but also magnetic behaviour. A closer understanding of laser-induced processes in metallic glasses can be effectively obtained by studies employing Mössbauer spectrometry [2–5] which provides simultaneous information on structural arrangement and magnetic microstructure.

Investigations performed upon $Fe_{78}B_{13}Si_9$ [2], Fe–B–Si–C [3], and Fe–B–Si–C and Fe–Ni–Mo–B [4] metallic glasses have revealed the effects of laser beams on the structure of magnetic domains. In amorphous alloys with positive magnetostriction, magnetic moments rotate out of the ribbon plane [2, 3] while in those with smaller magnetostriction they adopt random orientation [4]. In fully crystallized $Fe_{78}B_{13}Si_9$ alloys, laser treatment caused surface amorphization to a depth of about 100 nm [2]. Surface, as well as bulk, crystallization of metallic glasses was reported after employing different types of lasers with high-energy fluences [5].

The present study was initiated with the aim of unveiling laser-induced modifications of the magnetic structure in amorphous materials having a Curie temperature close to room temperature. The reason for this was twofold. Firstly, such materials do not show six-line Mössbauer patterns. Consequently, the line-intensity ratios, which are correlated to magnetic textures in [2–5], cannot be used as a measure of laser-induced structural modifications. It is noteworthy that changes in relative intensities of magnetically split Mössbauer spectral lines are governed mainly by internal stresses in the sample and that is why they directly depend on the magnetostriction (in sign and value) of the material. Thus, in the case of a small magnetostriction, possible changes in magnetic microstructure might be overlooked if one concentrates only on this parameter.

The second reason for choosing an amorphous alloy with a low magnetic ordering temperature takes into consideration the possibility of altering the magnetic structure by partial crystallization [6]. The formation of fine crystalline grains with a size of several nanometres, which are embedded in a residual amorphous matrix, can be easily controlled by the composition of the master amorphous alloy and the conditions of annealing [7]. Thus, the effects of laser treatment on both the crystalline and the amorphous structure can be simultaneously studied.

2. Experimental details

The amorphous $Fe_{76}Mo_8Cu_1B_{15}$ alloy was produced in the form of ribbons (6 mm wide and 20 μm thick) by the method of planar-flow casting. The complete amorphous state of the ribbons was confirmed by x-ray diffraction (XRD) and Mössbauer spectroscopy and no traces of crystallites were found in the as-quenched specimens.

Laser treatments were performed by a XeCl excimer laser (Siemens XP2020) operating in a pulse mode (pulse duration 55 ns, wavelength 308 nm, frequency 1 Hz). The laser beam was focused through a fly-eye homogenizer, in order to obtain a uniform intensity distribution

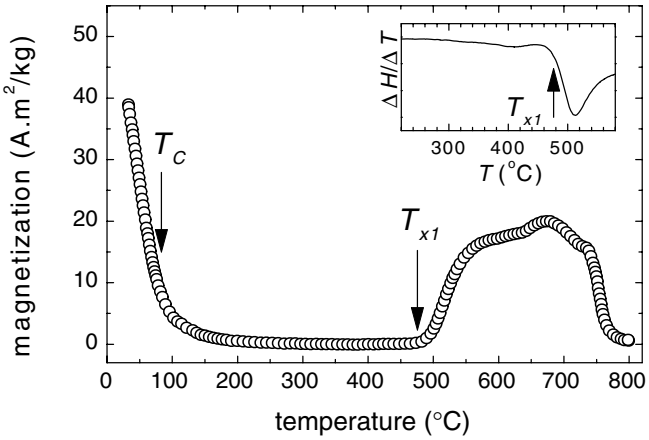

Figure 1. Thermomagnetic curve of the as-quenched $Fe_{76}Mo_8Cu_1B_{15}$ alloy. The Curie temperature T_C and the temperature of the onset of crystallization T_{x1} are indicated by arrows. The inset shows a DSC curve of the same alloy.

over a spot of 5×5 mm^2. Details on the laser beam characteristics can be found elsewhere [1]. Amorphous and nanocrystalline samples were treated by varying the number of pulses with an average laser fluence H up to 3 J cm^{-2} in a high-purity nitrogen atmosphere ($N_2 > 99.99\%$). The irradiation chamber was first evacuated to a residual pressure lower than 10^{-3} Pa and then filled with pure nitrogen to a pressure of 0.1 MPa.

XRD was performed in a (Bragg–Brentano) $\Theta/2\Theta$ geometry using Cu–K_α radiation (Bruker AXS). The Curie temperature and the crystallization temperature were derived from the temperature dependence of magnetization (300–1050 K) obtained by VSM-magnetometry. The crystallization behaviour was studied by differential scanning calorimetry (DSC) (Perkin Elmer).

Room temperature ^{57}Fe Mössbauer spectra were collected simultaneously in transmission geometry (TM) and by detecting conversion electrons (CEMS) with an escape depth of about 150 nm. CEMS measurements were performed at the dull side of the ribbons. A ^{57}Co/Rh source (activity $\approx$220 MBq) was mounted in a constant acceleration drive. Spectral parameters were refined by the NORMOS DIST program [8]. Calibration was performed by α-Fe and isomer shifts are given relative to this α-Fe.

3. Results and discussion

3.1. Characterization of crystalline and magnetic structure

The temperature dependence of the magnetization for amorphous $Fe_{76}Mo_8Cu_1B_{15}$ is presented in figure 1. The arrows indicate the Curie temperature, $T_C \approx 70$ °C, and the temperature of the onset of crystallization, $T_{x1} = 475$ °C, which is associated with a nucleation and growth of a new phase. The crystallization kinetics was verified by DSC and the same value of T_{x1} has been obtained as illustrated by the inset in figure 1. Annealing of the as-quenched alloy at a temperature above the first crystallization peak for one hour resulted in the formation of a crystalline phase. Using XRD, the observed phase was identified as bcc-Fe. Decomposition of the (110) reflection in figure 2 provided an estimation of the amount of bcc-Fe nanograins of about 40% with an average size of about 6 nm.

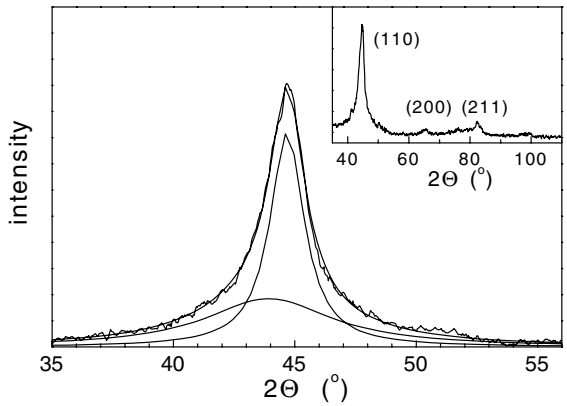

Figure 2. Decomposition of the (110) XRD reflection of the nanocrystalline $Fe_{76}Mo_8Cu_1B_{15}$ alloy into two components representing the amorphous and the crystalline phases. The inset shows the whole x-ray diffractogram.

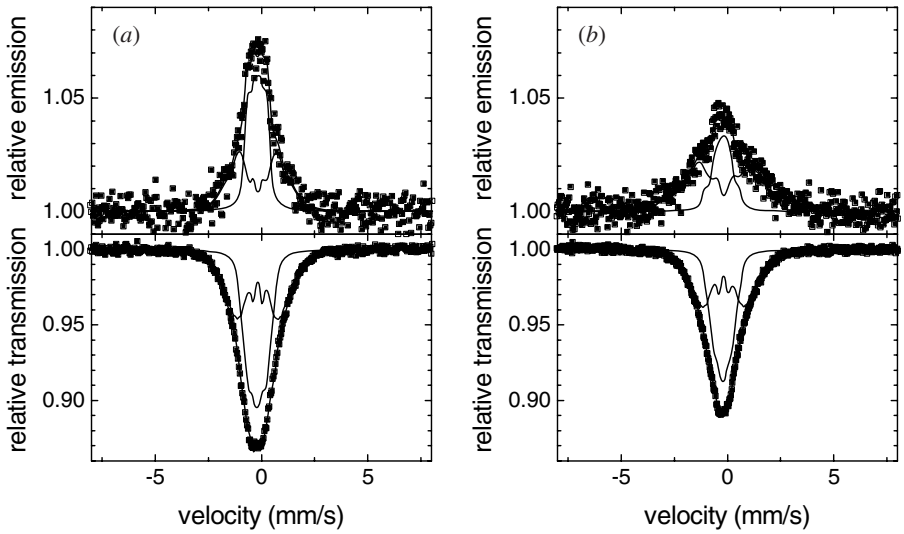

Figure 3. CEM (top) and TM (bottom) spectra including spectral components of the as-quenched $Fe_{76}Mo_8Cu_1B_{15}$ alloy: (*a*) untreated; (*b*) after laser treatment with 64 pulses at a fluence of 3 J cm^{-2}.

The broadened transmission and conversion electron Mössbauer spectra in figure 3(*a*) confirm the amorphous nature of the as-quenched alloy. They show combined electric quadrupole and magnetic dipole interactions characteristic for magnetic structures in the vicinity of the magnetic ordering transition. As seen in the CEM spectrum in figure 3(*a*), even the surface regions are fully amorphous. The spectra were evaluated by employing distributions of the quadrupole splitting $P(\Delta)$ and distributions of the hyperfine magnetic field $P(B)$ with a linear coupling to isomer shifts ($IS = a \times B + b$). Spectral components are also given in the figure. Their relative areas are nearly equal (the relative fractions of the magnetic component A_B are 47 and 52% for CEMS and TMS, respectively) which indicates a homogeneous occurrence of magnetic and non-magnetic structural positions of the resonant atoms. The error in the determination of spectral line areas is $\pm 2\%$.

The average values $\langle\Delta\rangle$ and $\langle B\rangle$ derived from the corresponding distributions are 0.59(3) mm s^{-1}, and 9.0(4) T, respectively, for CEMS and 0.681(5) mm s^{-1} and 8.54(7) T, respectively, for TMS. Magnetic fields are slightly prevailing in surface regions whereas the bulk of the sample depicts the higher influence of non-magnetic arrangements.

3.2. Laser treatment of the as-quenched alloy

3.2.1. General features of the Mössbauer spectra. The Mössbauer spectra obtained for the laser-treated as-quenched $Fe_{76}Mo_8Cu_1B_{15}$ alloy are shown in figure 3(*b*). For this sample we used 64 pulses with the energy density $H = 3$ J cm^{-2} applied to each irradiation spot on the dull side of the ribbon. Pronounced changes are detected in the magnetic microstructure of the surface regions. The CEM spectrum is notably broadened as compared with that of the untreated, as-quenched sample. The average magnetic hyperfine field was increased to $\langle B\rangle = 12.2(4)$ T and so was the relative fraction of the magnetic component $A_B = 65\%$. Non-magnetic regions were also affected but not to such a high extent ($\langle\Delta\rangle = 0.65(5)$ mm s^{-1}).

The same increasing tendency after laser treatment was also identified using TMS, yielding $\langle B\rangle = 8.96(7)$ T, $A_B = 54\%$, and $\langle\Delta\rangle = 0.643(5)$ mm s^{-1}. The detected changes between untreated and laser-treated specimens are, however, more delicate than those observed by CEMS. We can conclude that the laser beam affects mostly surface regions. Indeed, the melting depth caused by a homogenized laser beam was found to extend less than 1 μm below the surface [1]. In this respect, the CEMS technique is more appropriate. Nevertheless, bulk properties comprising magnetic arrangements are also influenced by laser treatment mostly due to a reorientation of magnetic domains by internal stresses [2–5]. As we demonstrate here, laser-induced structural modifications can also be revealed by TMS of not fully magnetic amorphous alloys.

Two mechanisms responsible for the observed changes can be considered: (i) internal stresses introduced via the melted and subsequently quenched surface; and (ii) changes in chemical and/or topological short-range order (SRO) of both the surface and the bulk of the ribbon. The laser beam acts as a source of intense heat which creates a plasma above the irradiated surface. As a consequence, atoms from the surrounding atmosphere (nitrogen in our case) are incorporated into the material. This effect, known as nitriding, is particularly strong in iron-based alloys and steels with ordered structure [1].

As far as the second proposed mechanism is concerned, excess heat created on the surface propagates further into the bulk thus causing relaxation and structural rearrangement of constituent atoms in the disordered structure, an effect which can hardly be observed in ordered crystalline materials. Thus, in addition to surface stresses it is also structural rearrangement that influences the bulk. Nevertheless, the alteration of the SRO is particularly strong in surface regions.

The as-quenched $Fe_{76}Mo_8Cu_1B_{15}$ alloy was treated by a homogenized laser beam with the energy densities of 1, 2 and 3 J cm^{-2}. We have used 16, 32 and 64 pulses per irradiation spot, four spots covering the whole area of one sample. In the following we shall inspect the role of the number of laser pulses per spot and the energy density of the beam on the SRO modifications.

3.2.2. Effect of the number of laser pulses. Figure 4 exhibits the CEM spectra of the as-quenched alloy. They belong to samples irradiated with the indicated number of laser pulses with an energy density of 1 J cm^{-2}. The shapes of spectral lines indicate deviations in SRO.

Quantitative features comprising average values of $P(\Delta)$ and $P(B)$ distributions, $\langle\Delta\rangle$ and $\langle B\rangle$, respectively, as well as the relative fraction A_B of the latter, are compiled in figure 5 for

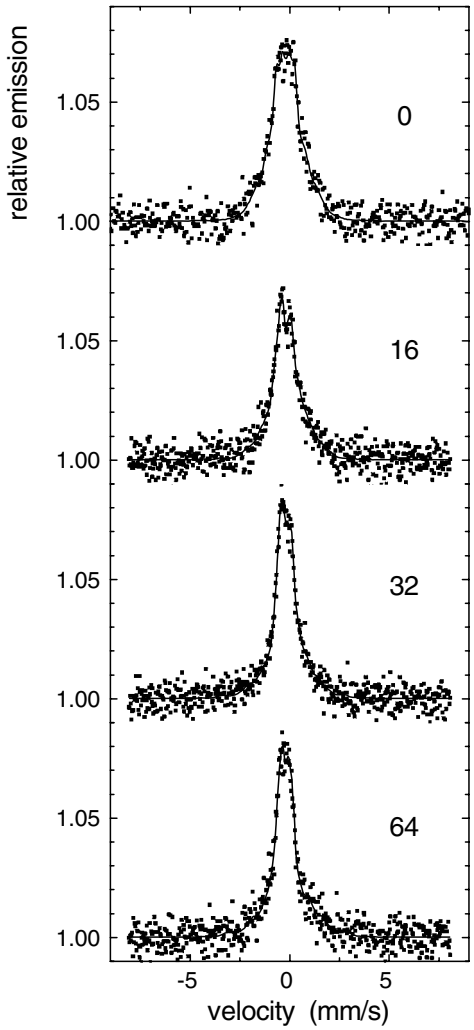

Figure 4. CEM spectra of as-quenched $Fe_{76}Mo_8Cu_1B_{15}$ alloys after laser treatment with the indicated number of pulses at a fluence of 1 J cm^{-2}.

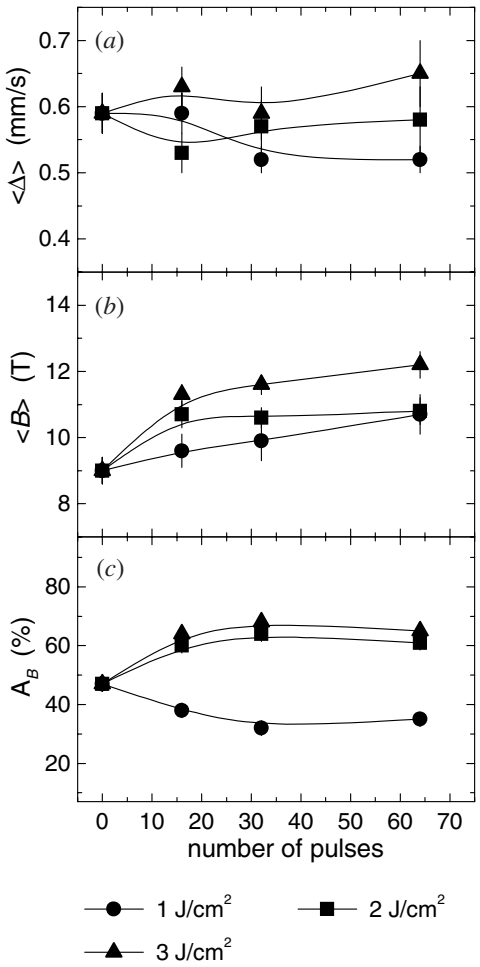

Figure 5. (*a*) Average value of $P(\Delta)$ distribution, $\langle\Delta\rangle$, (*b*) average value of $P(B)$ distribution, $\langle B\rangle$, and (*c*) relative area of magnetic component, A_B, plotted against the number of laser pulses at fluences of 1 J cm^{-2} (circles), 2 J cm^{-2} (squares) and 3 J cm^{-2} (triangles).

energy densities of 1, 2 and 3 J cm^{-2}. $\langle\Delta\rangle$ and A_B show a decrease for $H = 1$ J cm^{-2}. A slight decrease with a subsequent return to the original value is observed for $\langle\Delta\rangle$ and $H = 2$ J cm^{-2}. At other energy densities these parameters increase in value with the rising number of laser pulses. $\langle B\rangle$ increases monotonically with the number of pulses for all energy densities.

TM spectra have revealed a moderate increase in $\langle B\rangle$ and A_B with the rising number of laser pulses. Changes are, however, not so pronounced as on the surface. We can conclude that, with the rising number of laser pulses per irradiation spot, the average value of the hyperfine magnetic field increases regardless of the energy densities even though a decrease in the relative fraction of the magnetic regions is found for $H = 1$ J cm^{-2}.

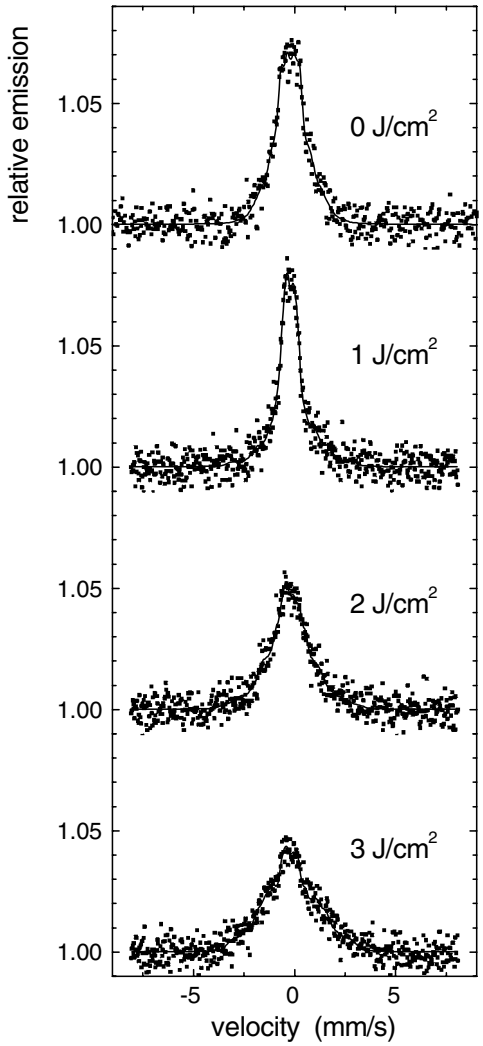

Figure 6. CEM spectra of as-quenched $Fe_{76}Mo_8Cu_1B_{15}$ alloys after laser treatments at the indicated energy density using 64 pulses.

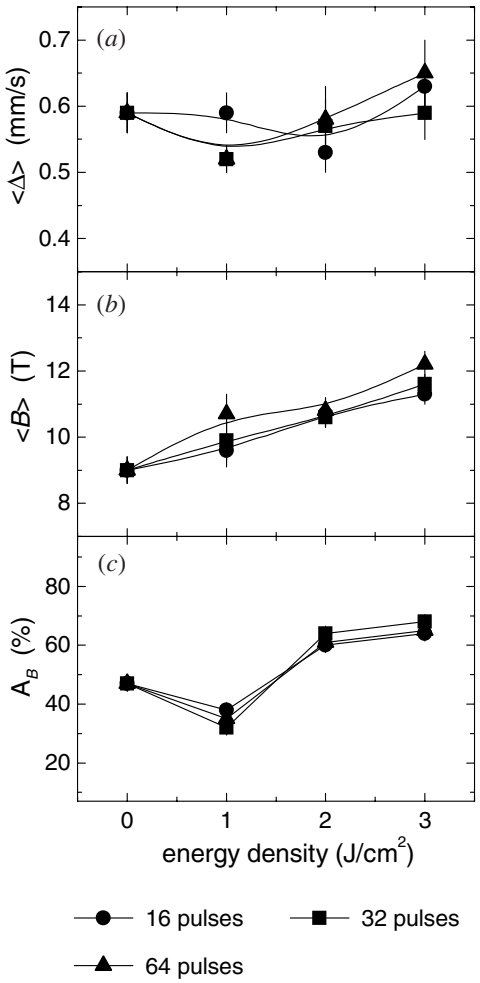

Figure 7. (*a*) Average value of $P(\Delta)$ distribution, $\langle\Delta\rangle$, (*b*) average value of $P(B)$ distribution, $\langle B\rangle$, and (*c*) relative area of magnetic component, A_B, plotted against the energy density of the laser beam, applying 16 (circles), 32 (squares) and 64 (triangles) pulses.

3.2.3. Influence of the energy density CEM spectra, along with distributions of hyperfine parameters in figure 6, correspond to the as-quenched alloy treated by 64 laser pulses with the indicated energy densities H. The average values of the distributions, $\langle\Delta\rangle$ and $\langle B\rangle$, and the relative fraction of the magnetic component, A_B, are plotted against H in figure 7 for 16, 32 and 64 pulses.

The average value of the hyperfine magnetic field $\langle B\rangle$ gradually increases as a function of H for any number of pulses. The same behaviour is also revealed from the TM spectra (not shown) even though the differences observed are not so pronounced. They are, nevertheless, higher than the error range. It is noteworthy that the relative fraction of the magnetic component is lower for $H = 1$ J cm^{-2} than in the as-quenched alloy.

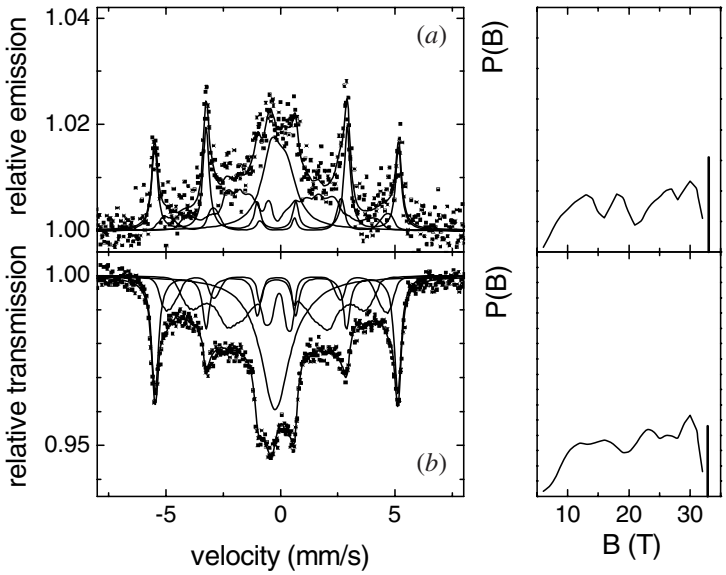

Figure 8. (*a*) CEM and (*b*) TM spectra including spectral components of nanocrystalline and untreated $Fe_{76}Mo_8Cu_1B_{15}$ alloys. The corresponding distributions of hyperfine magnetic fields $P(B)$ and hyperfine fields of the crystalline component (vertical lines) are plotted alongside each figure.

Paramagnetic regions characterized by the $P(\Delta)$ distributions display first of all a slight decrease and/or flattening, then a moderate increase of $\langle\Delta\rangle$ values with H. The complex behaviour of both $P(\Delta)$ and $P(B)$ indicates pronounced structural changes in the SRO. As a result, the magnetic microstructure is also affected. An increase of the Curie temperature due to the rearrangement of constituent atoms can be expected. No traces of crystalline phases were detected.

3.3. Laser treatment of the nanocrystalline alloy

The nanocrystalline $Fe_{76}Mo_8Cu_1B_{15}$ alloy shows a completely different Mössbauer pattern from the as-quenched one. CEM and TM spectra in figure 8 feature narrow lines superimposed to broadened components with a pronounced central part. The former are ascribed to the bcc-Fe crystalline phase whereas the latter belong to a residual amorphous matrix. A broad central peak/dip indicates that the amorphous remainder contains paramagnetic regions in which Fe atoms have preferentially non-magnetic nearest neighbours. The relative fraction of the paramagnetic component is smaller than that of the as-quenched alloy (about 25%) suggesting an increase in the Curie temperature. Such behaviour is often observed in nanocrystalline alloys and it is ascribed to penetrating exchange interactions from ferromagnetic bcc grains into the retained amorphous phase [9].

We have used one sextet of Lorentzian lines to reproduce the crystalline phase and two independent $P(B)$ distributions plus one broadened doublet to refine spectral parameters of the amorphous and interface regions. Partial subspectra can also be seen in figure 8. Details on the fitting procedure can be found elsewhere [10, 11]. It should be noted that interface regions contain resonant atoms located at the surface of nanograins as well as in their immediate vicinity. The resulting overall $P(B)$ distributions are plotted together with hyperfine fields of the bcc crystalline component (thick vertical line) in the right-hand panels of figure 8.

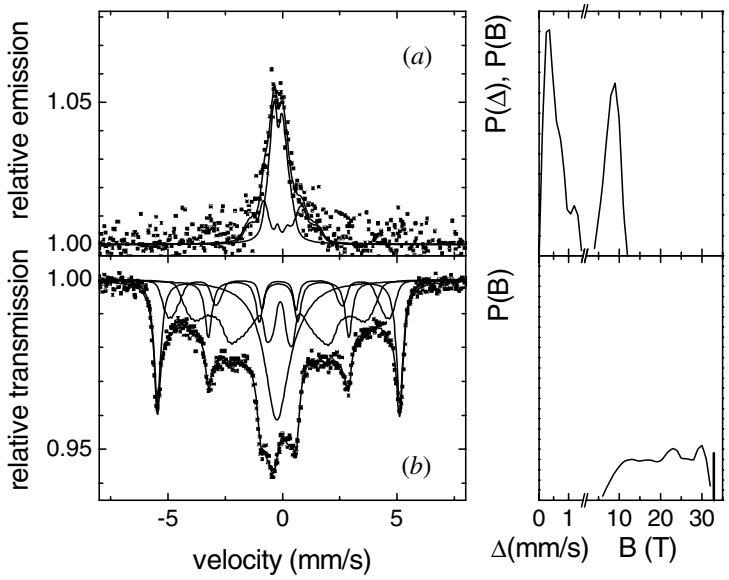

Figure 9. (*a*) CEM and (*b*) TM spectra including spectral components of the nanocrystalline $Fe_{76}Mo_8Cu_1B_{15}$ alloy after laser treatment with one laser pulse at a fluence of 1 J cm^{-2}. The corresponding distributions of hyperfine magnetic fields $P(B)$ and hyperfine fields of the crystalline component (vertical lines) are plotted alongside each figure.

The Mössbauer spectra of the nanocrystalline untreated alloy contain 23 and 31% of the narrow crystalline component for TMS and CEMS, respectively. Considering a contribution of interfacial regions, the total amount of crystallites can be estimated to be of 36 and 41%, correspondingly. The latter value represents the amount of nanograins in surface regions and it is in good agreement with the findings from XRD.

For ^{57}Fe Mössbauer spectra, the ratio of the second (fifth) to the third (fourth) line intensity is related to the direction of the net magnetic moment and varies between 4 and 0 for a parallel and a perpendicular orientation of the moment with respect to the plane of a ribbon-shaped sample, respectively. A random distribution of magnetic moment orientations gives the line-intensity ratio of 2. The magnetic components in TM and CEM spectra show a tendency of magnetic moments to turn into the ribbon plane on the surface as indicated by the higher line-intensity ratio in CEMS (1.13(4) versus 3.68(4)). This is mainly due to the formation of closure domains [2].

Mössbauer spectra of the nanocrystalline alloy after laser treatment with one pulse and $H = 1$ J cm^{-2} are illustrated in figure 9 together with the respective distributions of hyperfine fields and individual spectral components. TMS in figure 9(*b*) show almost the same pattern as the untreated specimen in figure 8(*b*). The amount of crystallites is practically unchanged (35%). Deviations are observed, however, in the orientation of magnetic moments in the bulk of the sample. The line-intensity ratio of 1.38(4) suggests that the moments are rotated into the ribbon plane as compared with those of the nanocrystalline untreated sample. This is the opposite behaviour from that reported for fully amorphous systems [2–5] and it can be explained by negative magnetostriction of the crystalline phase.

The CEM spectrum in figure 9(*a*) illustrates drastic changes in the surface SRO after laser treatment. The contribution of the paramagnetic doublet (not shown in $P(B)$, only in the Mössbauer spectra) was more than doubled from 28% in TMS to 63% in CEMS. On

the other hand, the crystalline phase has almost vanished. This is a consequence of surface melting due to the laser beam and subsequent rapid quenching due to the thermal contact with neighbouring regions of the material. Nearly complete surface re-amorphization after laser treatment of originally fully crystalline $Fe_{78}B_{13}Si_9$ ribbons was reported [2].

Low fields dominate in the $P(B)$ distribution in figure 9(a). Thus, the amorphous matrix adopts a similar structural arrangement as laser-irradiated as-quenched alloys. Consequently, the CEM spectrum was fitted with $P(\Delta)$ and $P(B)$ distributions. In addition, the retained amorphous phase shows a dramatic decrease in the strength of magnetic regions as compared with the nanocrystalline untreated specimen. $\langle B \rangle$ decreased from 17.4(5) T observed in the latter to 8.2(4) T after laser irradiation. This is primarily caused by the disappearance of nanocrystallites with high hyperfine magnetic fields (about 33 T) and exchange interactions among them. The influence of the amount of bcc-Fe nanograins on the magnetic microstructure of the amorphous matrix were studied in a similar $Fe_{80}Mo_8X_1B_{12}$ (X = Cu, Au) system [12] and the same behaviour was observed. It is noteworthy that the relative content of the magnetic disordered component was nearly unchanged (31% before, compared with 37% after laser treatment).

4. Conclusions

This (preliminary) study aimed to shed some light on laser-induced modifications of melt-spun metallic glasses, which do not exhibit strong magnetic interactions at room temperature. One of the goals was to verify the sensitivity of Mössbauer spectral parameters that are not related to magnetic texture (namely the line-intensity ratio) to reflect changes in structural and/or magnetic rearrangements caused by laser treatment. For that purpose we have employed both the transmission technique and the detection of conversion electrons.

The as-quenched $Fe_{76}Mo_8Cu_1B_{15}$ alloy, which was chosen as a model system in this study, shows nearly equal portions of magnetic and non-magnetic regions. The Curie temperature of this alloy was determined to be about 70 °C and the amorphous alloy starts to crystallize at 475 °C.

After laser treatment, the magnetic component was enlarged at the expense of the non-magnetic one. The average value of the hyperfine magnetic field distribution increases with the number of laser pulses applied per irradiation spot as well as with the energy density of the laser beam. For a low-energy density of 1 J cm^{-2}, the increase in $\langle B \rangle$ as a function of the number of pulses is not accompanied by an increase in the relative fraction of the magnetic component, as observed for irradiation with $H > 1$ J cm^{-2}. This result suggests that the sole 'quantitative' increase (i.e. relative fraction) of regions with magnetic dipole interactions cannot explain this seemingly controversial behaviour. Along with internal stresses generated by the excess heat of the laser beam, we have to take into consideration the SRO rearrangement of constituent elements. Here, Mössbauer spectrometry plays an unmatched role by providing the distributions of respective spectral parameters as quadrupole splitting and/or hyperfine magnetic field.

Both transmission and CEMS experiments gave the same results. The former, however, showed more delicate distinctions in the parameters studied. The laser-induced material modification was, as expected, more pronounced on the surface. In this respect, the CEMS technique seems to be more appropriate.

The laser treatment of the nanocrystalline $Fe_{76}Mo_8Cu_1B_{15}$ alloy has induced much more pronounced differences between the surface and the bulk. The crystalline bcc-Fe phase present in the sample previously was completely removed from the surface regions at least to the depth of 150 nm as evidenced by CEM spectra. On the other hand, no additional crystallization and/or

crystalline phases were observed as a result of laser irradiation under the present treatment conditions. The effects of surface melting and re-amorphization of nanocrystalline alloys deserve closer investigation.

Acknowledgments

This work was performed under the grants Franc/Slov/1 and SGA no 1/8305/01. MM is indebted to Deutscher Akademischer Austauschdienst (DAAD) for financial support during his stay in Göttingen. DSC was performed courtesy of Dr S Schneider (I. Physikalisches Institut, University of Göttingen).

References

[1] Schaaf P 2002 *Prog. Mater. Sci.* **47** 1–161
[2] Gonser U and Schaaf P 1991 *Fresenius J. Anal. Chem.* **341** 131–5
[3] Sorescu M 2000 *J. Appl. Phys.* **87** 5855–7
[4] Sorescu M 2000 *Phys. Rev.* B **61** 14 338–41
[5] Sorescu M 2000 *J. Magn. Magn. Mater.* **218** 211–20
[6] Suzuki K, Makino A, Inoue A and Masumoto T 1991 *J. Appl. Phys.* **70** 6232
[7] Suzuki K 1999 *Mater. Sci. Forum* **521** 312–14
[8] Brand R A, Lauer J and Herlach D M 1983 *J. Phys. F: Met. Phys.* **13** 675–83
[9] Hernando A and Kulik T 1994 *Phys. Rev.* B **49** 7064
Suzuki K and Cadogan J M 2000 *J. Appl. Phys.* **87** 7097
[10] Miglierini M and Grenèche J-M 1997 *J. Phys.: Condens. Matter* **9** 2303–19
[11] Miglierini M, Škorvánek I and Grenèche J-M 1998 *J. Phys.: Condens. Matter* **10** 3159–76
[12] Miglierini M, Tóth I, Seberini M, Illeková E and Idzikowski B *J. Phys.: Condens. Matter* submitted